Biochemical and Biophysical Research Communications **254,** 231–242 (1999)
Article ID bbrc.1998.9921, available online at http://www.idealibrary.com on IDEAL®

Induction of Nitric Oxide Synthase mRNA by Shear Stress Requires Intracellular Calcium and G-protein Signals and Is Modulated by PI 3 Kinase

Adel M. Malek,* Lianwei Jiang,† Ike Lee,‡ William C. Sessa,§ Seigo Izumo,‡ and Seth L. Alper†
**Department of Neurosurgery, Brigham & Women's Hospital, Children's Hospital and Harvard Medical School, Boston, Massachusetts 02115; †Molecular Medicine and Renal Units, and ‡Cardiovascular Division, Beth Israel Deaconess Medical Center, and Harvard Medical School, Boston, Massachusetts 02215; and §Department of Pharmacology, Boyer Center for Molecular Medicine, Yale University School of Medicine, New Haven, Connecticut 06536*

Received November 27, 1998

We have investigated the signaling pathways by which shear stress induces accumulation of endothelial nitric oxide synthase (eNOS) mRNA in bovine aortic endothelial cells (BAEC). Steady laminar fluid shear stress (20 dyn/cm^2) induced a time-dependent increase in eNOS mRNA levels that did not require *de novo* protein synthesis and was in part transcriptional. Shear responsiveness was conferred on a luciferase reporter by a portion of the eNOS gene promoter encoding the 5′-flanking region between nt −1600 and −779. Shear-mediated induction of eNOS mRNA was abolished by chelation of intracellular calcium ($[Ca^{2+}]_i$) with BAPTA-AM, and inhibited by blockade of calcium entry with SKF96535. In contrast, eNOS mRNA upregulation by shear was potentiated by thapsigargin-mediated depletion of $Ca^{2+}{}_i$ stores. Pertussis toxin (PTX) inhibited both the shear-induced elevation in $[Ca^{2+}]_i$ and the subsequent increase in eNOS mRNA, implicating a PTX-sensitive G-protein in both responses. Shear-induced upregulation of eNOS mRNA was unaffected by the calmodulin inhibitor W-7 and by the tyrosine kinase inhibitor herbimycin A, suggesting that neither calmodulin nor tyrosine kinases are required. However, eNOS mRNA upregulation was potentiated by the PI 3-kinase inhibitors wortmannin and LY294002, suggesting that PI 3-kinase inhibits the shear response. Although microtubule integrity is required for the shear-induced regulation of endothelin-1 mRNA and the morphological and cytoskeletal responses to flow, neither microtubule dissolution with nocodazole nor microtubule stabilization with taxol altered shear-induced $[Ca^{2+}]_i$ elevation or upregulation of eNOS mRNA. In conclusion, shear stress of BAEC increases eNOS transcriptional rate and upregulates eNOS mRNA levels by a process that requires calmodulin-independent $[Ca^{2+}]_i$ signaling and a PTX-sensitive G-protein, is inhibited by PI 3-kinase, and is independent of microtubule integrity and tyrosine kinase activity. © 1999 Academic Press

Key Words: **G-proteins; calcium; Fura-2; mechanotransduction; flow; kinases; mechanical stress.**

Abbreviations used: BAEC, bovine aortic endothelial cells; BAPTA-AM, bis-(o-aminophenoxy)-ethane-N,N,N′,N′-tetraacetic acid, tetra(acetoxymethyl)-ester; CHX, cycloheximide; LY249002, 2-(4-morpholinyl)-8-phenyl-4H-1-benzopyran-4-one; PI 3-kinase, phosphatidylinositol 3-kinase; TK, tyrosine kinase.

Expression of endothelial nitric oxide synthase (eNOS) is exquisitely sensitive to prevailing shear stress both *in vivo* (1) and *in vitro* (2, 3) (see (4), (5), and (6) for recent reviews). eNOS mRNA levels increase in direct proportion to shear duration and magnitude by a process sensitive to the inhibitor of transcription, actinomycin D, and to the K^+ channel blocker, tetraethylammonium, but not to the PKC inhibitors calphostin C and H-7 (3), or to the NOS inhibitor, L-NMA (2). Shear stress rapidly increases cytoplasmic calcium concentration ($[Ca^{2+}]_i$) (7, 8) by both ATP-dependent (9, 10) and independent processes (8, 11) and rapidly activates the heterotrimeric G-protein α subunits, $G_{q0/\alpha11}$ and $G_{\alpha i3/\alpha0}$ (12, 13). In addition, shear regulates the tyrosine phosphorylation state of several proteins (14, 15), including *src,* paxillin, and FAK, and increases eNOS serine and threonine phosphorylation by a tyrosine kinase-dependent step (16, 17). We have previously shown that shear stress-mediated endothelial cell alignment and actin stress fiber induction is dependent on both $[Ca^{2+}]_i$ and tyrosine kinase (TK) activity (18).

In addition to the upregulation of eNOS gene expression, flow induces a rapid increase in NO release in a biphasic manner; the early phase (<15 min) is dependent on the rate of change of shear (19), on Ca^{2+} and calmodulin, and on a PTX-insensitive G-protein(s). The later phase is dependent on shear stress magnitude

0006-291X/99 $30.00
Copyright © 1999 by Academic Press
All rights of reproduction in any form reserved.

and independent of Ca^{2+} and calmodulin (20), and is similarly unaffected by PTX (21). NO production by flow has been reported to be independent of the actin cytoskeleton but potentiated by microtubule disruption (22). Although independent of $[Ca^{2+}]_i$, the release of NO requires tyrosine kinase activity, is abolished by staurosporine, the PKC inhibitor calphostin C, and by Na^+/H^+ antiporter blockade using HOE694 (15). Recently, shear stress has been shown to increase the association of eNOS with the endothelial cytoskeletal (Triton X100-insoluble) fraction (23). The association of eNOS with caveolin may interfere with the association of eNOS with calmodulin, and may thus control eNOS activity (24, 25). We have examined the mechanism by which shear upregulates eNOS mRNA levels, focusing on evaluation of shear stress-sensitive signaling pathways. We present data suggesting critical roles for Ca^{2+} signaling, PTX-sensitive G-protein(s), and PI 3-Kinase activity.

MATERIALS AND METHODS

Materials. All reagents used were of the highest available grade. Cycloheximide, wortmannin, HOE694, and nocodazole were obtained from Sigma Chemicals (St. Louis, MO). BAPTA-AM was purchased from Molecular Probes (Eugene, OR). Pertussis toxin, SKF96365, LY294002, Calphostin C, and taxol were obtained from Calbiochem. Herbimycin A was purchased from Gibco-BRL (Gaithersburg, MD).

Cell culture. BAE cells (passage 6-15) were harvested from descending thoracic aortas obtained from the local abattoir by collagenase digestion. Greater than 98% of the resulting cells displayed uptake of Ac-LDL (Biomedical Technologies Inc., Stoughton, MA). The cells were cultured at 37°C, 5% CO_2 in a humidified incubator in growth medium consisting of Dulbecco's modified Eagle (DME) medium (Gibco-BRL) supplemented with 10% fetal calf serum (Gibco), 4 mM L-glutamine, 25 mM Hepes pH 7.4, 10 units/ml of penicillin, and 10 μg/ml of streptomycin. BAE cells were depolarized by exposure to a modified DME medium in which 135 mM NaCl was replaced by equivalent KCl.

Shear stress apparatus. A cone-plate viscometer purpose-built for the exposure of BAEC monolayers grown on commercial tissue culture plates was used as previously described (26). A cone of 1° angle was used at a steady rotational frequency of 5 rev/s to obtain a mean shear stress magnitude of 20 dyn/cm^2.

RNA isolation and hybridization. Total cellular RNA was isolated using RNeasy (Qiagen Inc., Los Angeles, CA). Northern blot hybridization was performed with QuickHyb solution from (Stratagene Inc., La Jolla, CA) with a random-primer ^{32}P-labeled (DECAprimeII kit, Ambion Inc., Austin, TX) 3.7 Kb EcoRI fragment of the bovine constitutive endothelial nitric oxide synthase (eNOS) (kindly provided by Dr. Thomas Michel, Brigham & Women's Hospital, Boston, MA), and a 1.3 Kb PstI fragment of the rat glyceraldehyde-3-phosphate dehydrogenase (GAPDH) cDNA. Following incubation, the blots were serially washed in 2X SSC-1% SDS and 0.2X SSC-1% SDS to a final temperature of 55°C for eNOS and at 63°C for GAPDH, then subjected to quantitative phosphorimager analysis (Molecular Dynamics, Sunnyvale, CA).

Promoter analysis. Subconfluent monolayers of BAE cells were transfected using Lipofectamine (Gibco-BRL) with a mixture of plasmid cDNAs encoding β-galactosidase (β-gal) under the transcriptional control of the RSV-promoter and one of two luciferase cDNAs. The F1 construct contained nt -1600 to $+22$ of the eNOS promoter, and the F4 construct contained nt -779 to $+22$ of the eNOS promoter (27). Transfected cells were allowed to reach confluence for 18 hours after which they were exposed to shear stress of 20 dyn/cm^2 for 18 hours. Cells lysates were then harvested and luciferase and β-gal activities were measured using commercially available kits (Kit#BC100L and kit#BL100P, Tropix Inc., Bedford, MA). Luciferase activity was normalized to β-gal activity to control for transfection efficiency.

Determination of cytoplasmic free calcium ion concentration ($[Ca^{2+}]_i$) using fura-2 ratio imaging. Fluorescence ratio imaging of intracellular free calcium concentrations using the indicator fura-2 AM was as previously described (28, 29). The method of shear stress exposure was as described by Ziegelstein *et al.* (30). Briefly, BAE cells were seeded inside glass capillary tubes, grown to subconfluency, and then incubated in growth media containing 2 μM Fura-2-acetoxymethyl ester (Fura-2 AM, Molecular Probes) for 30-40 min at 37°C in humidified 5% CO_2. The capillary tubes were then washed in a Ca^{2+}-measurement buffer (modified Hank's buffered saline solution) and mounted in a special chamber which enabled the steady pumping of laminar flow corresponding to 12 dyn/cm^2 on the inner surface of the microcapillary tube. $[Ca^{2+}]_i$ was measured in room air and at room temperature by fura-2 ratio imaging using an Image-1 digital ratio imaging system (Universal Imaging, Westchester, PA) equipped with an Olympus IMT-2 inverted microscope, a Dage-MTI CCD7 camera, a Genesys image intensifier, a Pinnacle REO-650 optical disk drive, and color video-printer. Fura-2 fluorescence was monitored in cells growing along the capillary tube face adjacent to the microscope objective. Images were acquired at 510 nm emission with alternating excitation at 340 and 380 nm at programmed intervals during 15-20 min periods. 340/380 ratio images of individual cells calculated on a pixel-by-pixel basis were recorded to optical discs for data processing. Fura-2 ratio values were calibrated *in vitro* to free Ca^{2+} concentrations ranging from 0 nM to 39.8 μM (Calcium Calibration Buffer Kit #2, Molecular Probes) using the same imaging parameters. K_d was determined by fitting the experimental R value at various free $[Ca^{2+}]$ using the equation $[Ca^{2+}]_{free} = K_d\,(S_{f2}/S_{b2})\,[(R - R_{min})/(R_{max} - R)]$, where the factor S_{f2}/S_{b2} corrects for fura-2 ion sensitivity at 380nm. A similar procedure was used for *in situ* calibration, in which 2 μM of the nonfluorescent Ca^{2+} ionophore, 4-Br-A23187 (Molecular Probes), was used to collapse Ca^{2+} gradients during 15 min incubation of fura-2-loaded BAECs in a series of Ca · EGTA buffers with free $[Ca^{2+}]$ ranging from 36 to 1270 nM. K_d in these conditions was 224 nM. Although calculated values of resting $[Ca^{2+}]_i$ determined by *in vitro* and *in situ* calibration curve differed only slightly, $[Ca^{2+}]_i$ was calculated from the *in situ* calibration curve. Extracellular medium contained 1.27 mM $CaCl_2$. Images were stored to optical disks for subsequent replay and data sampling from 8-12 individual cells for each microcapillary tube.

Immunostaining. BAE monolayers were washed three times with phosphate-buffered saline (PBS), fixed with 3.7% formaldehyde in PBS for 15 min at 37°C, permeabilized in PBS containing 0.1% triton X-100 for 15 min, then washed in PBS. The fixed and permeabilized cells were then incubated with monoclonal anti-tubulin antibody (Boehringer-Mannheim, Indianapolis, IN) for 30 min in PBS containing 1% BSA, washed with PBS for 30 min, then incubated with anti-mouse Cy3-conjugated IgG secondary antibody (Jackson Laboratories, West Grove, PA) for 30 min in PBS containing 1% BSA, washed with PBS for 30 min and fixed with Möwiol (Calbiochem, San Diego, CA). Stained cells were visualized in an epifluorescence microscope (Olympus Model BH-2) and photographed with T-Max 400 film (Kodak, Rochester, NY).

Statistics. Data were expressed as mean ± SEM. Analysis of variance (ANOVA) was used in conjunction with a Tukey-Kramer HSD correction test for all comparison pairs except as noted when the unpaired Student's *t* test was used. Statistical significance was

assumed for $p < 0.05$. Each set of experiments contained a matched control with n = 3-5 within each category.

RESULTS

Steady laminar fluid shear stress increases eNOS mRNA expression in a time-dependent fashion. To determine the optimal conditions for evaluation of the eNOS mRNA response to flow, we chose an arterial magnitude of shear stress under steady laminar flow using a cone-plate viscometer and confluent BAE monolayers. Northern blot analysis of total RNA collected at 0.5, 1, 2, and 6 hours showed a steady increase in eNOS mRNA, reaching 3-4 fold at six hours, without discernible change in GAPDH message (Fig. 1A). We chose six hours for subsequent signaling experiments to maximize signal-to-noise ratio.

Shear stress increases eNOS promoter activity. Previous work showed that actinomycin D abrogated the induction of eNOS mRNA by shear stress, implying a transcriptional mechanism. To determine whether the 5′-flanking region of the eNOS gene could confer shear-responsiveness, we undertook transient transfection experiments using luciferase reporter constructs containing portions of the eNOS promoter (Fig. 1B). Lysates of cells transfected with the F1 construct (−1600 to +22) showed a significant increase in normalized luciferase activity (3.31 ± 0.64 for shear vs 1.00 ± 0.39 for static, $p < 0.03$) comparable to the increase in eNOS mRNA. In contrast, BAE cells transfected with the F4 construct (−779 to +22) showed no statistically significant induction in response to shear (1.55 ± 0.36 for shear vs 1.00 ± 0.25 for static, p = n.s.). This finding suggests that the increase in eNOS mRNA expression is at least partially transcriptional, and that the shear stress response element (SSRE) for eNOS resides in the region between −1600 and −779 bp of the eNOS promoter.

Shear stress induction of eNOS mRNA does not require ongoing protein synthesis. Several cellular responses to shear stress require ongoing protein synthesis, including endothelial cell alignment, stress fiber induction, and sustained downregulation of ET-1 and PDGF-B mRNA levels at times > 4 h (18). We pretreated BAEC with cycloheximide (CHX, 10 μg/ml) to inhibit protein synthesis prior to onset of shear (Fig. 1C), and continued exposure during shear. Whereas CHX increased static levels of eNOS mRNA (1.70 ± 0.34) compared to control (1.00 ± 0.02, p = n.s.), shear in the presence of CHX further increased relative eNOS mRNA levels to 4.59 ± 1.26 ($p < 0.05$) compared to 3.11 ± 0.57 for shear without CHX ($p < 0.01$). Thus, the fold induction of eNOS mRNA by shear (3.1-fold) was not significantly affected by CHX (2.7-fold). This finding indicates that the mechanism of eNOS mRNA upregulation by shear differs from those of ET-1 and PDGF-B mRNA downregulation (31).

Pharmacological properties of shear stress-induced rapid intracellular calcium transients. To better define the possible role of $[Ca^{2+}]_i$ signaling in the induction of eNOS mRNA by flow, we measured $[Ca^{2+}]_i$ in Fura-2-loaded BAEC subjected to laminar shear stress (12 dyn/cm^2) in a glass capillary tube system. A step-stimulus of flow induced a nearly four-fold increase in $[Ca^{2+}]_i$ (400 ± 45% of the static value, $p < 0.01$) (Fig. 2). Pretreatment with the membrane-permeable Ca^{2+} chelator BAPTA-AM (30 μM) completely abolished the shear-induced $[Ca^{2+}]_i$ increase (107 ± 9% of the static value, p = n.s.) (Figs. 2A,B). Depletion of endoplasmic reticulum Ca^{2+} stores by pretreatment with the inhibitor of endoplasmic reticulum Ca^{2+}-ATPase, thapsigargin (3 μM), prior to onset of flow also significantly attenuated the increase in $[Ca^{2+}]_i$ (165 ± 7% of the static value, $p<0.05$). Exposure of BAEC to the store-operated Ca^{2+}/cation channel inhibitor, SKF965365 (50 μM) led to partial attenuation of the peak calcium transient (290 ± 25% of the static value, $p < 0.05$), suggesting that entry of extracellular Ca^{2+} also contributes to the shear-induced $[Ca^{2+}]_i$ transient.

Induction of eNOS mRNA by flow is dependent on $[Ca^{2+}]_i$ signaling and is blocked by endothelial depolarization. After characterizing the pharmacological properties of the shear-induced elevation of $[Ca^{2+}]_i$, we investigated its role in shear-induced upregulation of eNOS mRNA. BAPTA-AM (30 μM) pretreatment and co-incubation completely inhibited the upregulation of eNOS mRNA by shear stress (Fig. 3A). Whereas shear increased normalized eNOS mRNA levels from 1.00 ± 0.02 to 3.1 ± 0.57 ($p < 0.01$) in control cells, shear in the presence of BAPTA decreased eNOS mRNA levels from 1.57 ± 0.27 to 0.84 ± 0.10 ($p < 0.05$). Thapsigargin (3 μM) treatment decreased basal normalized eNOS mRNA levels from 1.00 ± 0.03 to 0.38 ± 0.04 ($p < 0.05$). Although thapsigargin had no effect on relative eNOS mRNA levels in sheared cells (2.85 ± 0.49) vs that in untreated sheared cells (2.99 ± 0.64, $p < 0.01$ vs unsheared cells), thapsigargin treatment increased the fold induction of eNOS mRNA by shear from 2.99 in untreated cells to 7.52 (Fig. 3B).

These findings suggest that release of calcium from intracellular stores relying on thapsigargin-sensitive Ca^{2+}-ATPases is not crucial for the induction of eNOS mRNA by shear stress. In contrast, whereas pretreatment of BAEC with the calcium channel inhibitor SKF96365 (50 μM) (32) only modestly inhibited Ca^{2+} entry (32), and was without effect on eNOS mRNA levels in static cells, the drug significantly inhibited shear-mediated fold-induction of eNOS mRNA (from 0.78 ± 0.11 to 1.65 ± 0.11). This 2.1-fold increase reflects statistically significant partial inhibition of the eNOS response to shear compared to that in untreated cells (Fig. 3B, $p < 0.05$). Exposure to the store-operated Ca^{2+} entry inhibitor, lanthanum chloride (11), for

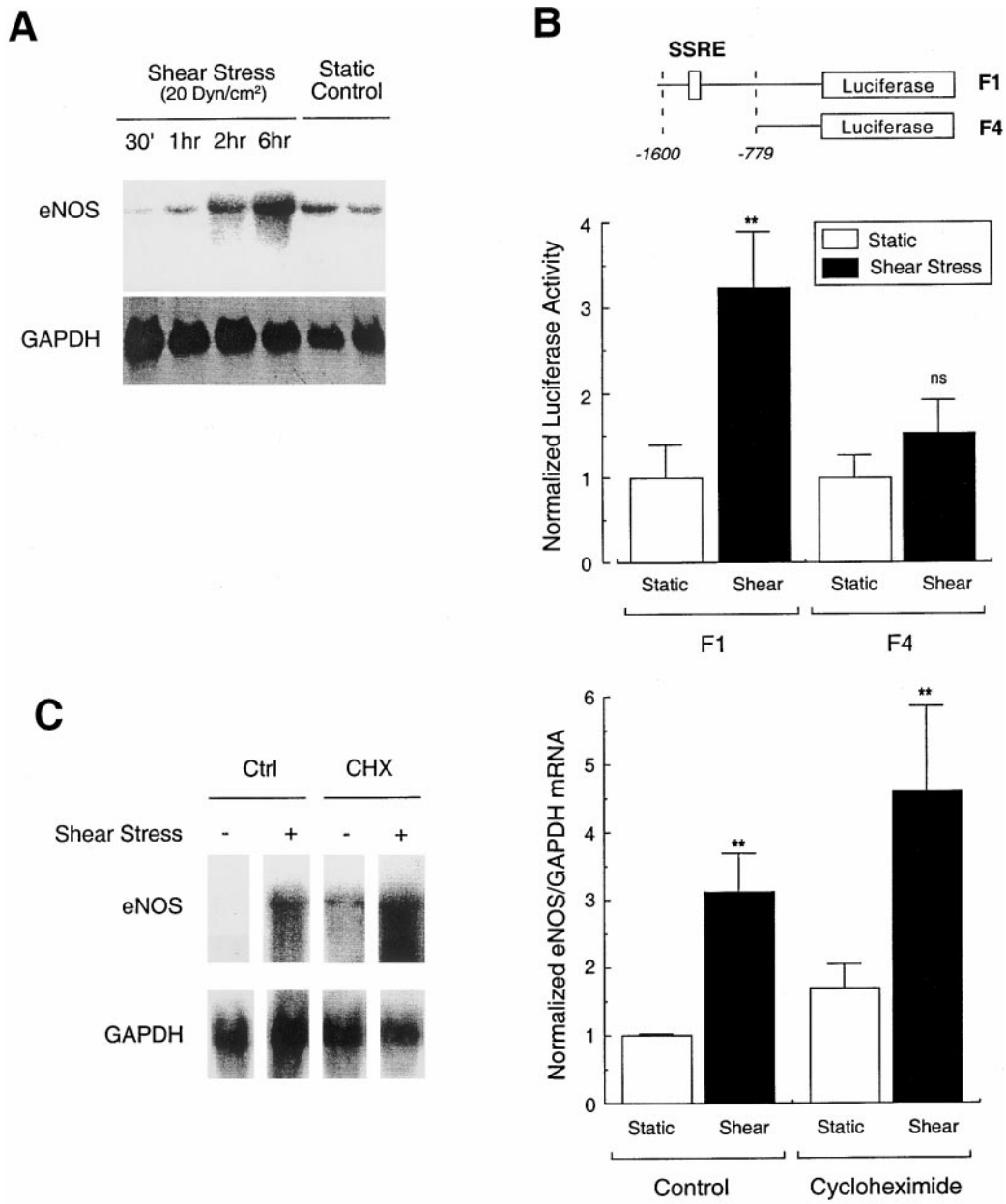


FIG. 1. Shear stress induces upregulation of eNOS mRNA in a time-dependent fashion by a partially transcriptional mechanism independent of *de novo* protein synthesis. (A) Northern blot analysis of total RNA from BAEC exposed to steady laminar fluid shear stress (20 dyn/cm^2) for 0.5, 1, 2, and 6 hours. Hybridization with radiolabeled bovine eNOS cDNA shows a time-dependent increase in mRNA, in the absence of increase in GAPDH mRNA. (B) Transcriptional activity of luciferase constructs containing nt −1600 to +22 (F1) and −779 to +22 (F4) of the eNOS promoter 5′-flanking region, normalized to (co-transfected) β-galactosidase activity. Only F1, but not the shorter F4 construct, confers shear responsiveness (*, $p < 0.05$). (C) The upregulation of eNOS mRNA by shear is independent of *de novo* protein synthesis, since it occurs in cells pretreated with cycloheximide (10 μg/ml) as shown by Northern blot analysis (left panel). Densitometric analysis from three separate experiments (right panel) (*, $p < 0.05$; **, $p < 0.01$).

longer than 3 hours was toxic to BAE monolayers, and BAE detachment prevented shear studies in EGTA-containing culture medium.

The previously reported shear-induced endothelial responses of hyperpolarization (33) via K^+-channel activation (34) prompted us to examine the consequences to eNOS mRNA levels of cell depolarization. Cell depolarization by 135 mM KCl completely inhibited the induction of eNOS mRNA (Fig. 3C), with shear increasing normalized eNOS mRNA levels from 0.89 ± 0.09 only to 1.20 ± 0.13 (p = n.s.) in contrast to the increase in control DME from 1.00 ± 0.05 to 2.30 ± 0.27 ($p < 0.01$). Thus, shear-induced upregulation of eNOS mRNA differs in this respect NO release induced by

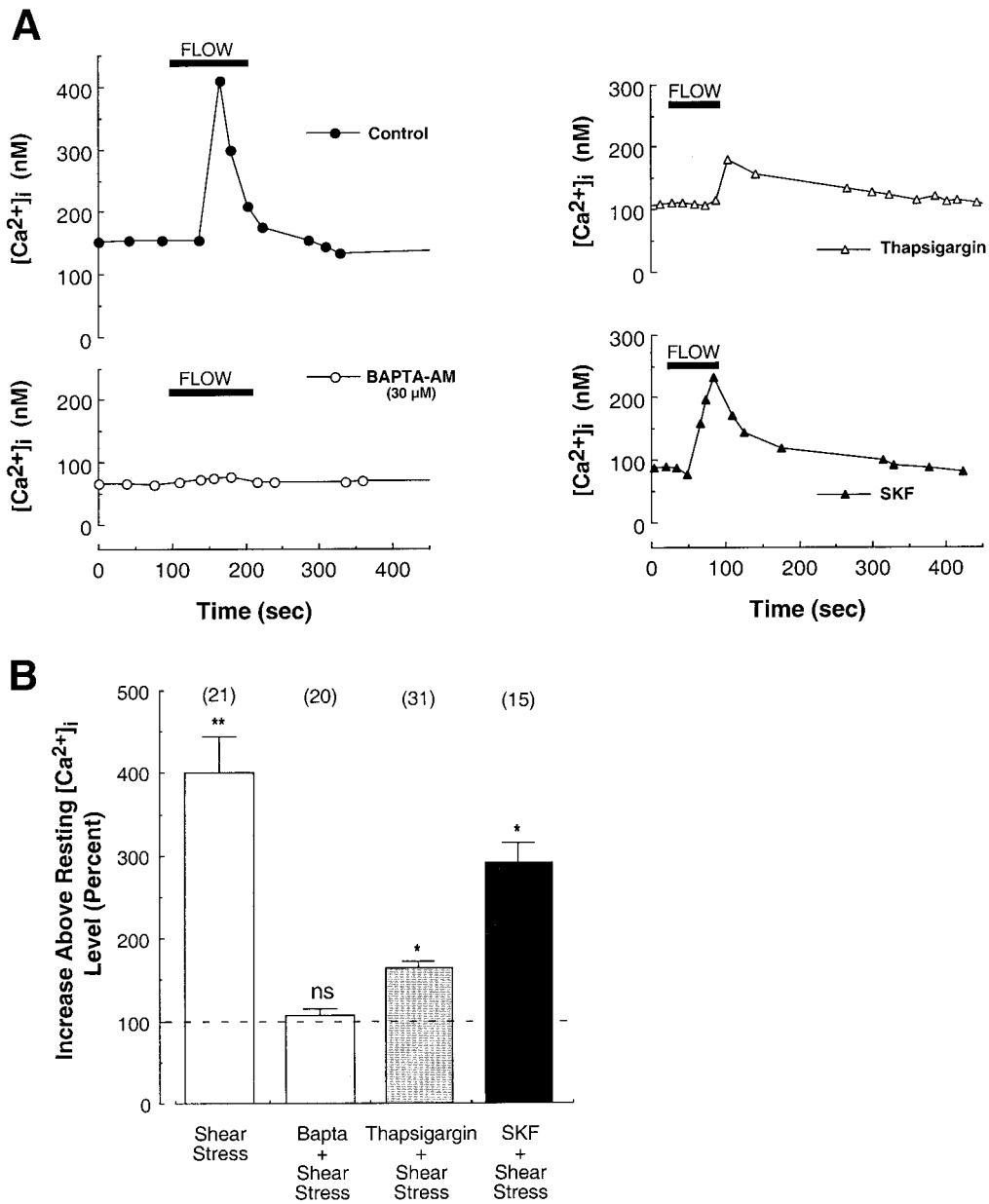


FIG. 2. Effect of calcium signaling modulators on shear-induced intracellular calcium response. (A) Typical BAEC $[Ca^{2+}]_i$ transients in response to a step increase in shear stress of 12 dyn/cm^2 (upper right, average of 8-12 cells from a single capillary; representative of 12 similar experiments). BAPTA-AM (30 μM) abolishes the rise in intracellular calcium induced by shear stress (lower right). Pretreatment with thapsigargin (3 μM) significantly attenuates the peak level of calcium in response to shear and also prolongs the recovery duration for return to baseline (upper right). A similar but less dramatic inhibitory effect is seen in response to pretreatment with SKF96365 (50 μM, lower right). (B) Bar graph of peak observed intracellular calcium levels observed during shear stress in the absence and presence of BAPTA-AM (30 μM), thapsigargin (3 μM), or SKF96365 (50 μM) (*, $p<0.05$; **, $p<0.01$), as described in Methods, (number of samples between parentheses).

flow or by bradykinin, in which instances membrane depolarization was without effect (35).

A pertussis-sensitive G-protein is involved in both $[Ca^{2+}]_i$ signaling and eNOS mRNA induction in response to shear. Heterotrimeric G proteins mediate or modulate many signaling pathways, and directly bind to and regulate gating of varied ion permeation pathways. To determine the possible involvement of $G\alpha_o/\alpha_i$-proteins in the induction of eNOS mRNA, we pretreated BAE cells with PTX (1 μg/ml) for six hours prior to shear stress to insure complete ADP-ribosylation as previously described by Gudi *et al.* (12, 13). We first evaluated the role of PTX-sensitive G-proteins on $[Ca^{2+}]_i$ signaling and found that PTX-

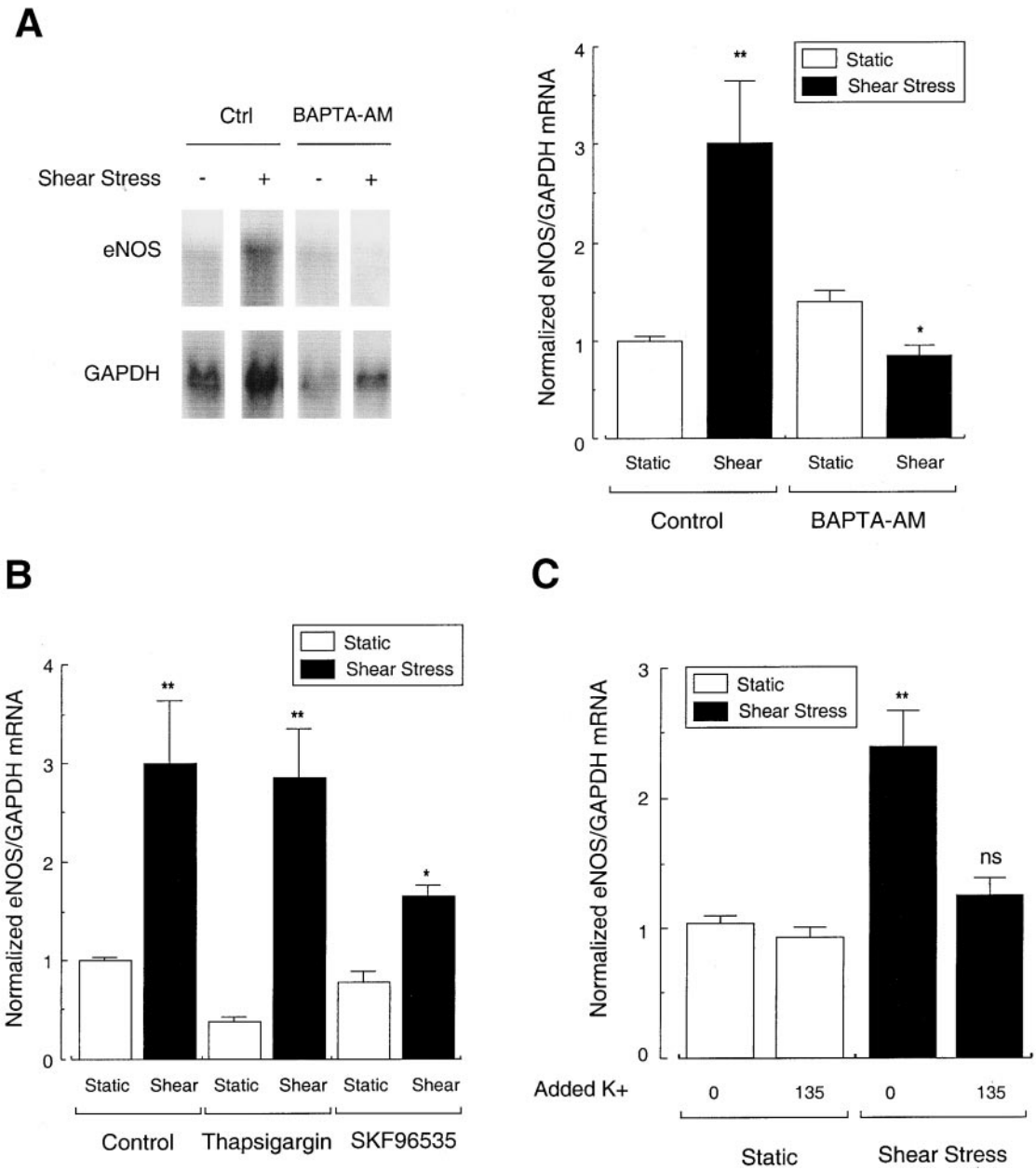


FIG. 3. Upregulation of eNOS mRNA by shear is abolished by intracellular calcium chelation, and by inactivation of a PTX-sensitive G protein. (A) Chelation of $[Ca^{2+}]_i$ by BAPTA-AM (30 μM) completely abrogates the induction of eNOS mRNA by shear stress as shown by Northern blot analysis (left panel) and by densitometric analysis of three separate experiments (right panel) (**, $p < 0.01$; *, $p < 0.05$). (B) Pretreatment with the inhibitor of endoplasmic reticulum Ca^{2+}-ATPases, thapsigargin (3 μM), to deplete calcium stores, lowered eNOS mRNA level in unsheared cells, but enhanced fold-activation by shear, leading to elevated levels in sheared cells (**, $p < 0.01$) similar to those in the absence of drug. Pretreatment with the calcium channel blocker SKF96365 (50 μM) attenuated but did not completely abolish eNOS mRNA increase by flow (*, $p < 0.05$). (C) BAE monolayers underwent plasma membrane depolarization by replacement of extracellular Na^+ by K^+, followed by exposure to shear stress while depolarizing conditions were maintained. The results show that depolarization using 135 mM $[K^+]_o$ abrogates eNOS mRNA induction by shear stress (**, $p < 0.01$).

pretreatment of BAE cells abrogated the shear-induced $[Ca^{2+}]_i$ transient (129 ± 15% of the static value, p = n.s.), suggesting that a PTX-sensitive G-protein is required for the shear-mediated $[Ca^{2+}]_i$ transient (Fig. 4A). We then evaluated the effect of PTX-pretreatment on eNOS mRNA induction, and found that it inhibited nearly completely the shear-induced increase of eNOS mRNA. Compared to untreated cells, in which shear increased relative eNOS mRNA levels from 1.00 ± 0.16 to 3.90 ± 0.44 (3.9-fold, $p < 0.01$), PTX pretreatment reduced induction by shear to 1.7-fold, increasing relative eNOS mRNA levels from 0.77 ± 0.03 to 1.34 ±

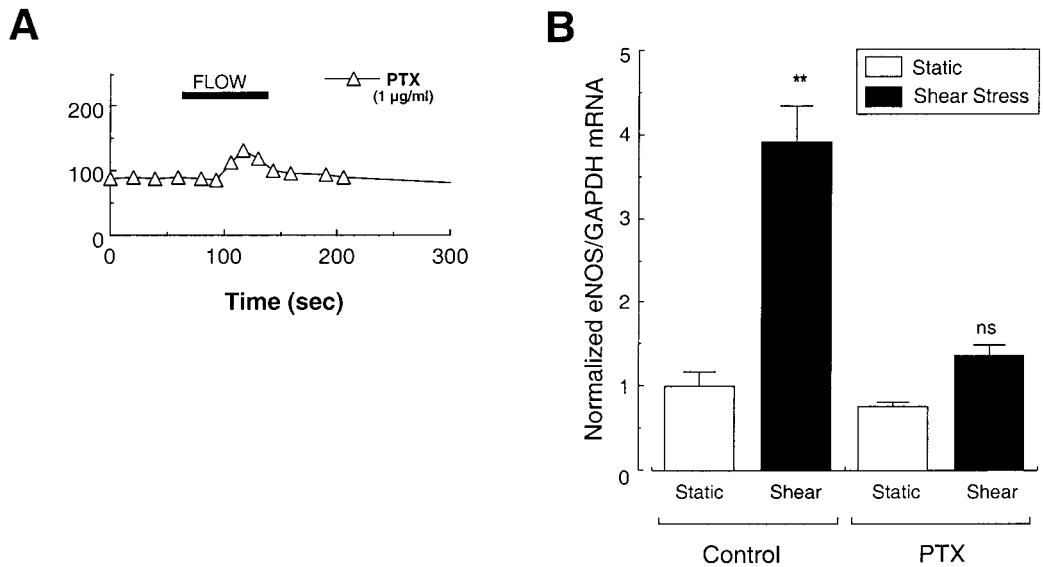


FIG. 4. Pertussis toxin inhibits both intracellular calcium increase and eNOS mRNA induction by shear stress. (A) Typical time course measurement of $[Ca^{2+}]_i$ transients in response to a step increase in shear stress of 12 dyn/cm^2. PTX (1 μg/ml) significantly inhibits the rise in intracellular calcium induced by shear stress. (B) Preincubation of BAE cell monolayers with pertussis toxin (1 μg/ml) inhibits the shear-activated induction of eNOS mRNA as shown by densitometric analysis of three separate experiments (**, $p < 0.01$).

0.15 (p = n.s. compared to static values in the absence of PTX) (Fig. 4B).

Inhibition of PI 3-Kinase potentiates upregulation of eNOS mRNA by shear stress. The association of PI 3-kinase with focal adhesion contacts and its putative role as a signaling mediator prompted tests of its role in eNOS mRNA upregulation by shear in the presence of wortmannin or LY294002. Under static conditions, PI 3-kinase inhibition with wortmannin (100 nM) doubled the level of normalized eNOS mRNA from 1.00 ± 0.10 to 1.95 ± 0.41 ($p < 0.05$). The normalized level of eNOS mRNA after shear increased further from 3.22 ± 0.39 ($p < 0.01$) in untreated cells to 11.0 ± 3.09 ($p < 0.01$) in wortmannin-treated cells, representing a significant, 75% increase in the fold-induction of normalized eNOS mRNA levels from 3.22-fold to 5.65-fold (Fig. 5A). To obtain further evidence for PI 3-kinase involvement in shear-induced eNOS mRNA upregulation, we compared the less potent PI 3-kinase inhibitor, LY294002 (36). Consistent with the effect of wortmannin, LY294002 (30 μM) similarly increased by 134% the fold-induction of eNOS mRNA by shear stress, from 3.22-fold to 7.52-fold ($n = 3$, $p < 0.05$). Taken together, these findings suggest that PI 3-kinase activity negatively modulates the upregulation of eNOS mRNA by shear stress.

Calmodulin action is unnecessary for upregulation of eNOS mRNA by shear. The important role of Ca^{2+}-calmodulin (CaM) in eNOS activation by displacing the inhibitory protein, caveolin (reviewed in (37)), prompted examination of the role of CaM activity in the upregulation of eNOS mRNA by flow. Although CaM has been implicated in the early NO release in response to changes in flow (20), CaM inhibition with W-7 (30 μM) had no significant effect on the induction of eNOS mRNA by shear (Fig. 5B). Shear increased normalized eNOS mRNA levels in control cells from 1.00 ± 0.4 to 4.04 ± 0.60 ($p < 0.01$) and in the presence of W-7 from 1.38 ± 0.28 to 6.23 ± 0.31 ($p < 0.01$); there was no significant difference in the fold induction (4.05 for control and 4.51 for W-7 treated cells). This finding is consistent with a previous report showing that the enhanced NO production induced by sustained flow is independent of calmodulin activity (20). Also consistent with previously reported data, we found that the protein kinase C (PKC) inhibitor, calphostin C (3). had no effect on the induction of eNOS mRNA by shear (3.10-fold for control vs 2.90-fold for calphostin C, p = n.s., data not shown).

Herbimycin-sensitive tyrosine kinase activity is not involved in the upregulation of eNOS mRNA by shear stress. Shear stress has been shown to induce activation of *src* and increased tyrosine phosphorylation of paxillin, and FAK. This response is crucial for activation of ERK1/2 (14) and for cytoskeletal and morphological remodeling in response to shear (18). To determine the role of increased tyrosine phosphorylation in flow-mediated upregulation of eNOS mRNA, BAEC monolayers were pretreated with herbimycin A (1 μM) for six hrs prior to application of shear stress (20 dyn/cm^2). In this set of experiments, shear increased normalized eNOS mRNA from 1.00 ± 0.02 to 2.68 ± 0.41 ($p < 0.01$) in untreated cells and from 1.14 ± 0.37 to 2.55 ± 0.46 ($p < 0.05$) in herbimycin A- pretreated

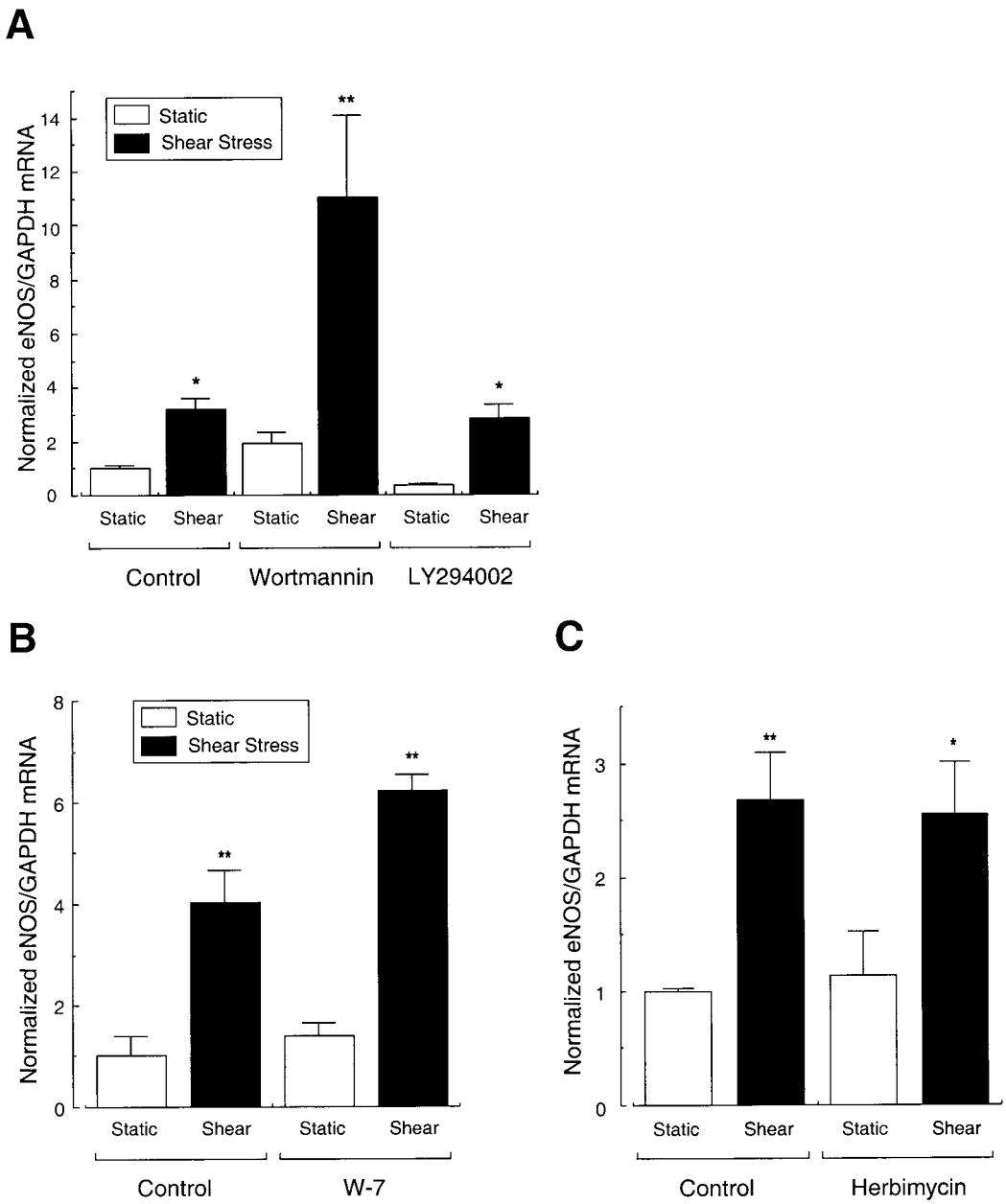


FIG. 5. Shear induction of eNOS mRNA is enhanced by PI 3-kinase inhibition but is unaffected by inhibitors of calmodulin and tyrosine kinase. (A) Inhibition of PI 3-kinase by wortmannin (100 nM) or by LY294002 (30 μM) each increased the fold-induction of normalized eNOS mRNA level by shear stress (**, $p < 0.01$; *, $p < 0.05$) as shown by densitometric evaluation of three separate experiments. (B) Inhibition of Ca/CaM kinase by W-7 (30 μM) did not significantly change baseline static eNOS mRNA levels and preserved responsiveness to shear stress, with an unchanged fold-induction (**, $p < 0.01$). (C) Inhibition of tyrosine kinase by herbimycin A (1 μM) affected neither baseline eNOS mRNA expression nor its upregulation in response to shear stress (*, $p < 0.05$; **, $p < 0.01$).

cells. As shown in Fig. 5C, the shear-induced fold-inductions did not differ significantly (2.67-fold vs 2.23-fold).

Microtubule network integrity is not required either for $[Ca^{2+}]_i$ increase or for eNOS mRNA induction by shear stress. The requirement of microtubule integrity for shear-induced endothelial cell alignment and shape changes (18) supported the hypothesis that the microtubule network (Fig. 6A, top panel) transmits, at least in part, externally applied mechanical stresses across the endothelial cell plasma membrane (38). To test the validity of this hypothesis for shear-induced upregulation of eNOS mRNA, microtubules were disrupted using nocodazole (10 μg/ml) resulting in dissolution of the fine microtubular network (Fig. 6A, middle panel), or were stabilized with taxol (10 μM) (Fig.

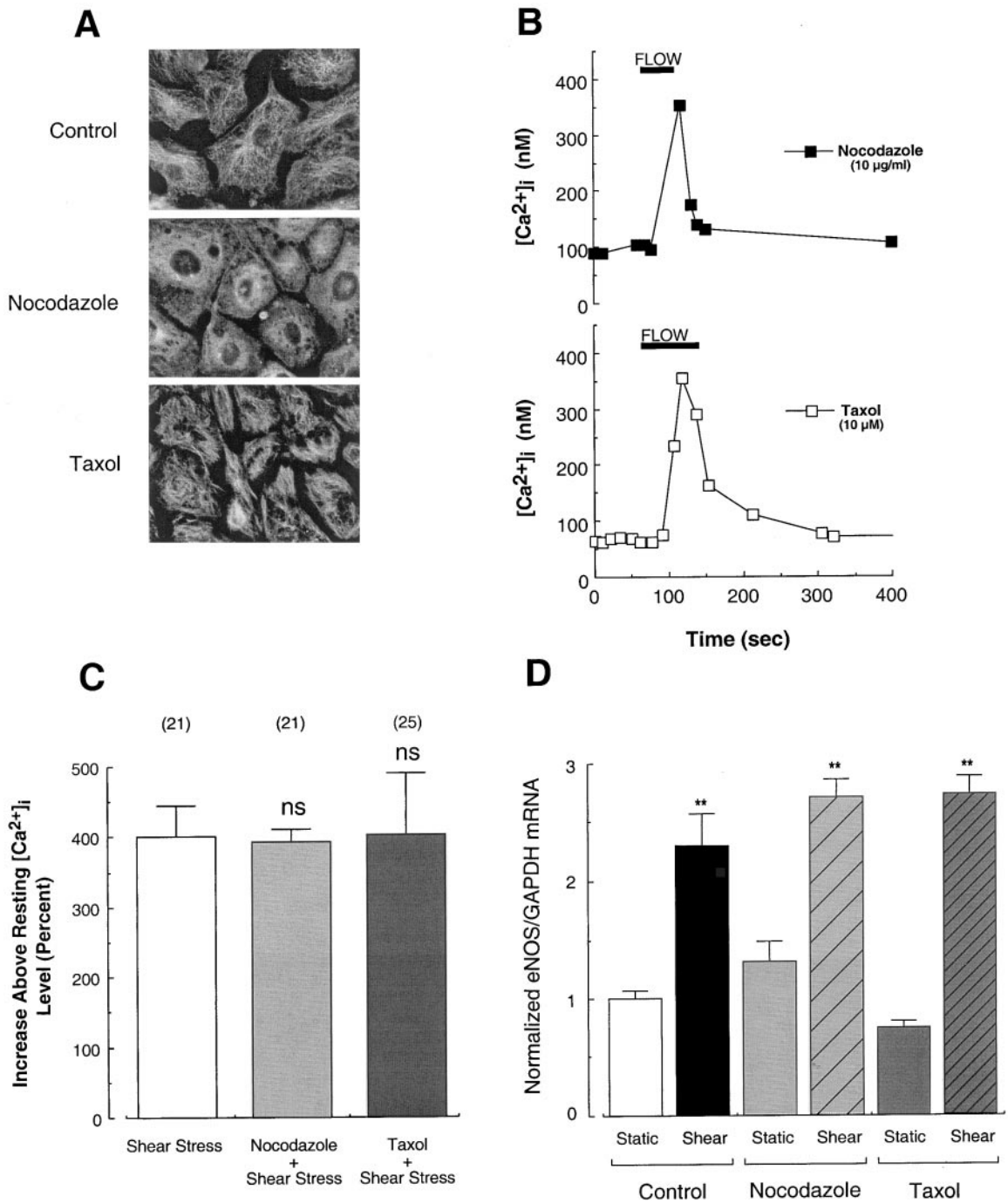


FIG. 6. Microtubules are involved in neither the shear-induced elevation of $[Ca^{2+}]_i$ nor in the resulting upregulation of eNOS mRNA level. (A) Tubulin immunostaining of confluent BAEC monolayers treated without (top panel) or with nocodazole (10 μg/ml, middle panel) or with taxol (10 μM, bottom panel). (B) Typical time course of cytoplasmic $[Ca^{2+}]_i$ measured with Fura-2 fluorescence ratio in BAEC pretreated with nocodazole or taxol. (C) Bar graph comparing the peak values of $[Ca^{2+}]_i$ measured in response to shear stress shows no significant modulation by microtubule disruption or stabilization, (number of samples between parentheses). (D) Bar graph showing fold-induction of eNOS mRNA by shear stress after pretreatment with nocodazole or taxol, revealing minimal effect of microtubule polymerization state on eNOS mRNA responsiveness to shear (**, $p < 0.01$).

6A, bottom panel) prior to applying flow. In untreated cells shear increased normalized levels of eNOS mRNA levels from 1.00 ± 0.07 to 2.31 ± 0.27 ($p < 0.01$) (Fig. 6B), whereas in nocodazole-treated cells it increased levels from 1.31 ± 0.17 to 2.71 ± 0.16 ($p < 0.01$), and in taxol-treated cells from 0.74 ± 0.06 to 2.74 ± 0.16 ($p < 0.01$). The fold-induction of normalized eNOS mRNA levels by shear was unchanged by nocodazole (2.31-fold

vs 2.06-fold, p = n.s.) but increased to 3.68-fold by taxol ($p < 0.05$). Neither nocodazole nor taxol pretreatments had significant effects on the shear-mediated increase in $[Ca^{2+}]_i$ (Fig. 6C,D).

DISCUSSION

Nitric oxide and its biosynthetic enzyme, eNOS, play critically important roles in the normal homeostasis and pathophysiology of the vessel wall including atherosclerosis. eNOS mRNA transcription and levels increase in response to chronic exercise (1) and were recently implicated in the remodeling process following surgically induced decrease in blood flow (39). Transient transfection using eNOS promoter reporter constructs showed that the F4 construct (nt −779 to +22) which contains the GATA and SP1 binding sites previously shown to confer basal transcription was not sufficient to confer shear responsiveness; this region also contains AP-1, AP-2, NF-1, CRE and sterol regulatory element sequences, although their functional activity remains to be demonstrated (27). The AP1 element mediates induction by shear stress of the MCP-1 gene (40, 41), and the SP1 element of the tissue factor gene mediates its induction by shear stress (42). However, neither of these suffice to mediate eNOS mRNA induction, since the F4 construct containing AP1, SP1, and GATA sites was insufficient to confer shear responsiveness.

In contrast, the eNOS gene promoter region between nt −1600 and −779, was sufficient to confer shear responsiveness. This region contains the SSRE consensus sequence, GAGACC, previously shown to mediate shear-activation of PDGF-B mRNA (43) via increased binding to NF-kappa-B p50-p65 heterodimers (41,44). However, two findings suggest that induction of the eNOS gene by shear stress is not mediated by its SSRE. First, eNOS mRNA was induced by shear in the presence of dexamethasone (2), which interferes with NF-kappa-B transactivation potential (45). Second, aspirin, which inhibits activation of NF-κ-B by preventing degradation of its inhibitor I-κ-B (46, 47), had no effect on induction of eNOS mRNA by shear (data not shown).

We have shown that the mechanism of eNOS mRNA regulation by flow diverges from those of acute NO release in response to flow. In contrast to flow-mediated NO release, eNOS mRNA induction was unaffected by inhibitors of calmodulin (20), tyrosine kinase (23), protein kinase C, and microtubules (22), but was blocked by KCl depolarization (35), and required $Ca^{2+}{}_I$ elevation (23) and active PTX-sensitive G-protein (21). Thus, chelation of $Ca^{2+}{}_I$ with BAPTA-AM prevented the shear-induced increase in eNOS mRNA level, consistent with a recent report (48). However, depletion of endoplasmic reticulum Ca^{2+} stores with thapsigargin, potentiated, rather than inhibited, the shear-induced increase in eNOS mRNA level, even while inhibiting most of the shear-induced elevation of $[Ca^{2+}]_i$.

This finding suggests that the eNOS mRNA induction by shear requires Ca^{2+} influx from the extracellular medium, a process potentiated by thapsigargin-depletion of intracellular Ca^{2+} stores with its consequent activation of store-operated Ca^{2+} channels of the plasma membrane (49). Although ionomycin-mediated Ca^{2+} influx failed to elevate eNOS mRNA levels in unsheared cells (48), the partial inhibition of shear-induced eNOS mRNA upregulation by SKF96365, an inhibitor of calcium entry by pathways other than voltage-gated Ca^{2+} channels (32), is consistent with this hypothesis. Inhibition of shear-induced eNOS mRNA upregulation by KCl-mediated membrane depolarization (reducing the electrical driving force for Ca^{2+} entry) further supports this hypothesis. The different responses of shear-induced eNOS mRNA levels to BAPTA, thapsigargin, SKF96365, and ionomycin, suggest that only some routes of Ca^{2+} entry impinge on this signaling pathway activated by shear. Selectivity of Ca^{2+} entry pathways has also been reported in hippocampal neurons undergoing activation of the transcription factor CREB via nuclear translocation of calmodulin [Deisseroth, 1998 #101]. Additional insight into distinct functional capabilities of the various Ca^{2+} entry pathways of endothelial cells may derive from the reported ability of thapsigargin to potentiate shear-induced generation and release of prostaglandin I_2 and NO (50).

Pretreatment of BAE cells with PTX abolished both the shear-induced acute elevation of $[Ca^{2+}]_i$ and the subsequent upregulation of eNOS mRNA level. These results suggest crucial roles for a PTX-sensitive G-protein(s) in both processes, and allow speculation that G-proteins may directly gate a Ca^{2+} permeability activated by shear. Recent experiments have shown that shear can directly activate PTX-sensitive and insensitive G-proteins both in endothelial cells and in membrane preparations (12). Further work has revealed that shear can increase GTPase activity of purified G-proteins in reconstituted membrane vesicles, in the absence of cytoskeletal protein, by a rapid (<1 sec) transmembrane process sensitive to membrane lipid composition (13).

These findings are consistent with the lack of requirement by shear-induced eNOS mRNA upregulation for microtubule integrity observed in the present study. Although the endothelial cytoskeleton can transmit externally applied stresses and has been shown to be structurally linked to the nucleus (62), it does not appear to play a necessary role in the shear-induced increase in $[Ca^{2+}]_i$ or in the upregulation of eNOS mRNA. This result contrasts with the central role of microtubules in shear-induced responses of cellular elongation and alignment and actin stress fiber

induction (18). The independence of eNOS mRNA induction from microtubules also differs from the requirement for integrity of microtubules for the short term upregulation (63) and long-term downregulation (unpublished data) of endothelin-1 mRNA level.

PI 3-kinase inhibition by wortmannin (100 nM) and by LY294002 (30 μM) each increased fold-induction of eNOS mRNA by shear, suggesting a possible inhibitory role for PI 3-kinase in this cellular response to shear. Recent studies have revealed synergistic roles for PI 3-kinase and PTX sensitive G-proteins in store-operated Ca^{2+} influx-mediated exocytosis in HL-60 granulocytes (65). Ca^{2+} influx and PI 3-kinase activity are both essential for ligand-stimulated internalization of the c-Kit receptor in DA-1 cells (66). Further work will be needed to determine the interactions, if any, between PI 3-kinase, shear-activated G-proteins, and calcium signaling (67) in the endothelial cell exposed to flow.

Previous studies using pharmacological inhibition of nitric oxide synthase have shown that flow-activated NO release is not required for subsequent shear-induced increase in eNOS mRNA level, thus ruling out an autocrine role for NO itself (2). Calmodulin inhibition using W-7 had no effect on eNOS mRNA upregulation, suggesting either the absence of or redundancy of feedback control mechanisms involving calmodulin (and, perhaps caveolin) in response to increased calcium in the regulation of eNOS mRNA induction (24, 25). Similarly, even though flow-mediated NO release has been shown to depend on intact tyrosine kinase activity (15), the latter was not critical in the eNOS mRNA induction by flow, despite increased shear-induced activation of *src* (17) and tyrosine phosphorylation of paxillin and FAK (14, 64), and the requirement of tyrosine kinase activity for shear-induced BAEC shape change and cytoskeletal remodeling.

In conclusion, we have shown that shear stress upregulates eNOS mRNA by a process which requires PTX-sensitive G-protein mediated $[Ca^{2+}]_i$ signaling, does not require thapsigargin-sensitive Ca^{2+} stores, and that may be under negative regulation by PI 3-kinase. Endothelial NOS mRNA induction is not tightly coupled to endothelial cell shape, cytoskeletal remodeling, or to endothelin-1 regulation, as it is unaffected by inhibitors of tyrosine kinase activity, and is independent of microtubule integrity. The mechanism of eNOS mRNA induction by shear also diverges from that involved in flow-mediated NO release in its independence from inhibition of protein kinase C, tyrosine kinase, and calmodulin activities. Further work is needed to delineate the potential interactions between shear-activated G-proteins, calcium signaling and PI 3-kinase activity in the eNOS mRNA response to shear.

ACKNOWLEDGMENTS

This work was supported by NIH grants P30-HL15157 and P60-DK34854 (A.M.M.), and by the Boston Neurosurgical Foundation to A.M.M. S.L.A. and S.I. are Established Investigators of the American Heart Association.

REFERENCES

1. Sessa, W. C., Pritchard, K., Seyedi, N., Wang, J., and Hintze, T. H. (1994) *Circ. Res.* **74,** 349–353.
2. Ranjan, V., Xiao, Z., and Diamond, S. L. (1995) *Am. J. Physiol.* **269,** H550–555.
3. Uematsu, M., Ohara, Y., Navas, J. P., Nishida, K., Murphy, T. J., Alexander, R. W., Nerem, R. M., and Harrison, D. G. (1995) *Am. J. Physiol.* **269,** C1371–1378.
4. Traub, O., and Berk, B. C. (1998) *Arterioscler. Thromb. Vasc. Biol.* **18,** 677–685.
5. Davies, P. F. (1997) *Atherosclerosis* **131**(Suppl.), S15–17.
6. Chien, S., Li, S., and Shyy, Y. J. (1998) *Hypertension* **31,** 162–169.
7. Ando, J., Ohtsuka, A., Korenaga, R., Sakuma, I., and Kamiya, A. (1993) *Front. Med. Biol. Eng.* **5,** 17–21.
8. Helmlinger, G., Berk, B. C., and Nerem, R. M. (1995) *Am. J. Physiol.* **269,** C367–375.
9. Dull, R. O., and Davies, P. F. (1991) *Am. J. Physiol.* **261,** H149–154.
10. Nollert, M. U., and McIntire, L. V. (1992) *J. Biomech. Eng.* **114,** 321–326.
11. Shen, J., Luscinskas, F. W., Gimbrone, M. A., Jr., and Dewey, C. F., Jr. (1994) *Microcirculation* **1,** 67–78.
12. Gudi, S. R., Clark, C. B., and Frangos, J. A. (1996) *Circ. Res.* **79,** 834–839.
13. Gudi, S., Nolan, J. P., and Frangos, J. A. (1998) *Proc. Natl. Acad. Sci. USA* **95,** 2515–2519.
14. Takahashi, M., and Berk, B. C. (1996) *J. Clin. Invest.* **98,** 2623–2631.
15. Ayajiki, K., Kindermann, M., Hecker, M., Fleming, I., and Busse, R. (1996) *Circ. Res.* **78,** 750–758.
16. Corson, M. A., James, N. L., Latta, S. E., Nerem, R. M., Berk, B. C., and Harrison, D. G. (1996) *Circ. Res.* **79,** 984–991.
17. Jalali, S., Li, Y. S., Sotoudeh, M., Yuan, S., Li, S., Chien, S., and Shyy, J. Y. (1998) *Arterioscler. Thromb. Vasc. Biol.* **18,** 227–234.
18. Malek, A. M., and Izumo, S. (1996) *J. Cell Sci.* **109,** 713–726.
19. Frangos, J. A., Huang, T. Y., and Clark, C. B. (1996) *Biochem. Biophys. Res. Comm.* **224,** 660–665.
20. Kuchan, M. J., and Frangos, J. A. (1994) *Am. J. Physiol.* **266,** C628–636.
21. Kuchan, M. J., Jo, H., and Frangos, J. A. (1994) *Am. J. Physiol.* **267,** C753–758.
22. Knudsen, H. L., and Frangos, J. A. (1997) *Am. J. Physiol.* **273,** H347–355.
23. Fleming, I., Bauersachs, J., Fisslthaler, B., and Busse, R. (1998) *Circ.Res.* **82,** 686–695.
24. García-Cardeña, G., Martasek, P., Masters, B. S., Skidd, P. M., Couet, J., Li, S., Lisanti, M. P., and Sessa, W. C. (1997) *J. Biol. Chem.* **272,** 25437–25440.
25. Michel, J. B., Feron, O., Sase, K., Prabhakar, P., and Michel, T. (1997) *J. Biol. Chem.* **272,** 25907–25912.
26. Malek, A. M., Gibbons, G. H., Dzau, V. J., and Izumo, S. (1995) *Meth. Cell Sci.* **17,** 165–176.
27. Zhang, R., Min, W., and Sessa, W. C. (1995) *J. Biol. Chem.* **270,** 15320–15326.

28. Husain, M., Bein, K., Jiang, L., Alper, S. L., Simons, M., and Rosenberg, R. D. (1997) *Circ. Res.* **80,** 617–626.
29. Husain, M., Jiang, L., See, V., Bein, K., Simons, M., Alper, S. L., and Rosenberg, R. D. (1997) *Am. J. Physiol.* **272,** C1947-C1959.
30. Ziegelstein, R. C., Cheng, L., and Capogrossi, M. C. (1992) *Science* **258,** 656–659.
31. Malek, A. M., and Izumo, S. (1994) *J. Hypertens.* **12,** 989–999.
32. Gorenne, I., Labat, C., Gascard, J. P., Norel, X., Nashashibi, N., and Brink, C. (1998) *J. Pharm. Exp. Ther.* **284,** 549–552.
33. Nakache, M., and Gaub, H. E. (1988) *Proc. Natl. Acad. Sci.* **85,** 1841–1843.
34. Olesen, S. P., Clapham, D. E., and Davies, P. F. (1988) *Nature* **331,** 168–170.
35. Gooch, K. J., and Frangos, J. A. (1996) *Am. J. Physiol.* **270,** C546–551.
36. Vlahos, C. J., Matter, W. F., Hui, K. Y., and Brown, R. F. (1994) *J. Biol. Chem.* **269,** 5241–5248.
37. Michel, T., and Feron, O. (1997) *J. Clin. Invest.* **100,** 2146–2152.
38. Ingber, D. E. (1997) *Annu. Rev. Physiol.* **59,** 575–599.
39. Rudic, R. D., Shesely, E. G., Maeda, N., Smithies, O., Segal, S. S., and Sessa, W. C. (1998) *J. Clin. Invest.* **101,** 731–736.
40. Shyy, J. Y., Lin, M. C., Han, J., Lu, Y., Petrime, M., and Chien, S. (1995) *Proc. Natl. Acad. Sci.* **92,** 8069–8073.
41. Lan, Q., Mercurius, K. O., and Davies, P. F. (1994) *Biochem. Biophys. Res. Comm.* **201,** 950–956.
42. Lin, M. C., Almus-Jacobs, F., Chen, H. H., Parry, G. C., Mackman, N., Shyy, J. Y., and Chien, S. (1997) *J. Clin. Invest.* **99,** 737–744.
43. Resnick, N., Collins, T., Atkinson, W., Bonthron, D. T., Dewey, C. F., Jr., and Gimbrone, M. A., Jr. (1993) *Proc. Natl. Acad. Sci.* **90,** 4591–4595.
44. Khachigian, L. M., Resnick, N., Gimbrone, M. A., Jr., and Collins, T. (1995) *J. Clin. Invest.* **96,** 1169–1175.
45. De Bosscher, K., Schmitz, M. L., Vanden Berghe, W., Plaisance, S., Fiers, W., and Haegeman, G. (1997) *Proc. Natl. Acad. Sci.* **94,** 13504–13509.
46. Weber, C., Erl, W., Pietsch, A., and Weber, P. C. (1995) *Circulation* **91,** 1914–1917.
47. Kopp, E., and Ghosh, S. (1994) *Science* **265,** 956–959.
48. Xiao, Z., Zhang, Z., and Diamond, S. L. (1997) *J. Cell. Physiol.* **171,** 205–211.
49. Gericke, M., Oike, M., Droogmans, G., and Nilius, B. (1994) *Eur. J. Pharmacol.* **269,** 381–384.
50. Macarthur, H., Hecker, M., Busse, R., and Vane, J. R. (1993) *Br. J. Pharmacol.* **108,** 100–105.